A CCII-Based Relaxation Oscillator as a Versatile Interface for Resistive and Capacitive Sensors

Shahid Malik[#], Tarikul Islam[*], S.A. Akbar[#]

[#]*Academy of Scientific & Innovative Research (AcSIR) -Central Electronic Engineering Research Institute (CSIR-CEERI), Pilani, India*

[*]*Department of Electrical Engineering, Faculty of Engineering and Technology, Jamia Millia Islamia University, New Delhi*

Abstract-- In this paper, a novel Current-Mode (CM) square/triangular wave oscillator, based on second generation current conveyor (CCII), operating as resistance/capacitance to time conversion is described. The proposed oscillator, which consists of two CCII as an active element, three grounded resistances and one capacitance found to be an effective alternate of voltage mode based interfaces for wide range capacitive and resistive sensors. The interface circuit was implemented with commercially available current feedback operational amplifier AD844 from Analog Devices and passive components. Experimental results confirmed the theoretical expectations, showing good linearity in wide oscillation frequency/period range, which can be independently adjusted through resistive or capacitive external passive components. Experimental measurement was also conducted on a fabricated capacitive humidity sensor to verify the real time application of the proposed interface circuit. The interface circuit has shown a good accuracy and linearity for wide variation in capacitance of humidity sensor.

Keywords— Relaxation oscillator; second generation current conveyor; CCII; sensor; Interface electronic circuit

I. INTRODUCTION

Oscillators are one of the most useful and very well known electronic circuit use to generate AC periodic waveforms (e.g., square-wave, triangular wave and sinusoidal waveform) [1]. They are used in a wide range of applications such as control systems, telecommunication and measurement systems. Nowadays, one of the most useful and interesting application of these oscillators is as an analog front end circuit for the resistive and capacitive sensors [2]. Typically, these oscillators are based on an Integrator (formed by an R-C cell) followed by a hysteresis comparator and implemented in Voltage-Mode (VM) approach using operational amplifiers (OA). In this way, these circuits provide an impedance to frequency conversion and can be used as an interface for resistive / capacitive sensors [2].

Most of the oscillator circuits are designed using VM based OA because of their simple design. However, the simplicity in design of circuits using a VM operational amplifier may turn into a disadvantage as far as their finite gain-bandwidth and low slew rates are concerned [1-2]. This problem can be tackled by properly substituting operational amplifier with second generation current conveyor (CCII) [3], the basic Current-Mode (CM) analog block, which shows high gain-bandwidth, high slew rate, high linearity, wide dynamic range, possibility of be designed with low power consumption and simple circuitry [2-3].

Various oscillator circuits has been realized with CCIIs. The present trend is to decrease the number of passive elements in the circuit with minimum active blocks. Several quasi digital solutions can be found in the literature using either a VM Schmitt trigger [4], designed using a voltage comparator and a pair of resistors or using a CM Schmitt trigger [5] designed using current feedback operational amplifier (CFOA) with a pair of resistors and capacitors. However, the former (i.e. VM Schmitt trigger) suffers from poor frequency stability and low slew rate of conventional commercially available OA. The latter solutions (i.e. CM Schmitt trigger) proposed in exhibits better frequency stability, but its oscillation frequency depends on the amplitude of square wave output signal, which in turn reduce estimation range. The other CM design proposed in [6], designed using an operational transconductance amplifier (OTA) and miller Integrator, perform capacitance to pulse width conversion, shows low sensitive to parasitic capacitance and temperature, but require a large number of active and passive components which increase the complexity and power consumption. Among the CM solutions using either OTA [6] or CCII [5-11] the CCII based design proposed in [9] found to be more effective and versatile for both resistive and capacitive sensors.

For these reasons, we propose a CM interface, implemented through a square/triangle wave oscillator, operating an impedance to period conversion (R-T and C-T), allow to neglect the effect of both CCII internal parasitic components and node saturations. In the proposed architecture, the effect of parasitic components on node X was strongly compensated by avoiding capacitive load, keeping only a resistive load of slightly higher value than parasitic component. Resultant, there are no limitations of higher estimation range; the proposed solutions are suitable for wide range capacitive sensor (e.g., humidity) and resistive sensor (e.g., gas) interface. Additionally, the interface sensitivity and measurement operating range can be easily set through some external passive components. Experimental measurement has been performed by implementing the scheme on prototype PCB using commercially available AD844 [12], as CCII and passive samples of capacitance and resistances. The experiment has also been performed to validate the interface electronic circuit for humidity sensing application. The capacitive humidity sensor based on γ-Al_2O_3 sensing film is fabricated in the lab using Dip-Coating Method. The sensing film is deposited in between inter-digital electrodes.

II. CCII Basic Theory

The current conveyor was first presented by Sedra and smith in 1968, represented as CCI [13]; however the effectiveness of current mode design was recognized only after the introduction of CCII [14], two years later than CCI Due to its unique and useful ways of realizing complex circuit functions, CCII is claimed to be the standard building block for current mode operation as far as analog signal processing applications are concerned [3].

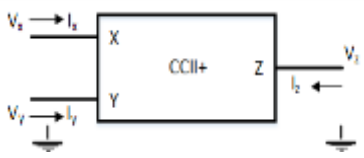

Fig.1. Schematic Symbol of CCII+

In an ideal CCII, whose schematic symbol is shown in Fig. 1, *X* node has zero impedance, whereas *Z* and *Y* node show infinite impedance. In CCII, if a current i_x is injected at *X* node, an equal current i_z will be obtained at node *Z* with direction either equal or opposite to current i_x, whereas if a voltage v_y is applied at node *Y*, an equal voltage v_x will be obtained at node *X*. The terminal characteristic of CCII is summarized in the following matrix representation.

$$\begin{bmatrix} i_x \\ v_x \\ i_z \end{bmatrix} = \begin{bmatrix} 0 & 0 & 0 \\ 1 & 0 & 0 \\ 0 & \pm\beta_i & 0 \end{bmatrix} . \begin{bmatrix} v_y \\ i_x \\ v_z \end{bmatrix} \quad (1)$$

The plus and minus signs of the current transfer ratio β_i In (1) indicates whether the conveyor is formulated as a non-inverting (positive) or inverting (negative) circuit, termed as CCII- or CCII+. In Fig. 1 positive is taken which means i_z and i_x both flowing simultaneously away or toward the conveyor.

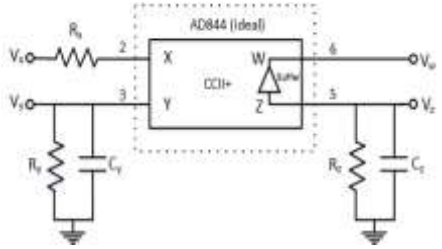

Fig. 2. IC 844with parasitic elements and a unity gain buffer

The salient features of CCII can be implemented using commercially available integrated circuits. Commercially available IC AD844 from analog devices is modelled as ideal positive CCII (CCII+), having parasitic input and output impedance, a unity gain buffer and a current gain of unity ($i_x = i_z$). The schematic diagram of AD844 with parasitic components is shown in Fig. 2, dotted line shows the ideal CCII with unity gain voltage buffer. The terminal characteristics of AD 844 can be described as

$$i_x = i_z,\ v_x = v_y,\ i_y = 0,\ v_w = v_z \quad (2)$$

The AD844 provides a distinct advantage over basic CCII+, having a low output impedance buffer between node Z and W which allows accessing the voltage of node Z without loading the transfer function. The typical values of parasitic components of AD844 are $R_z = 3M\Omega$, $R_y = 10M\Omega$, $R_x = 50\Omega$, $C_z = 4.5pF$ and $C_y = 2pF$.

III. The Proposed Circuit: Analysis and Simulation

The schematic block diagram of the proposed oscillator, employed as analog interface is shown in Fig. 3.The proposed circuit has designed in such a way that the effect of parasitic elements will be negligible. The influence of parasitic components of node X was is reduced by avoiding capacitive loads, keeping only a resistive load of slightly higher value than the parasitic resistance at the same terminal. The specific configuration of this circuit allows us to neglect the effect of parasitic components of node Y and Z in square/triangle wave generation. In fact the effect of parasitic capacitance at node Z was strongly compensated by utilizing the capacitive sensor element on that node. Resulting, there is no limitation for high frequency values and hence a wide measurement range (higher than 2.5 decades for capacitive sensor) can be obtained. It is possible to set the sensitivity and dynamic range of read-out circuit through external parameters. Fig. 4 shows the voltage signals at the main terminal of the interface.

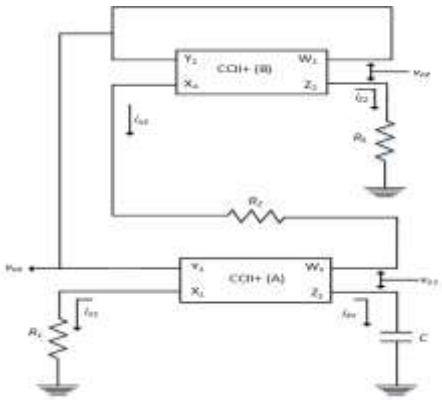

Fig. 3. Proposed Square/triangular wave generator with CCII+

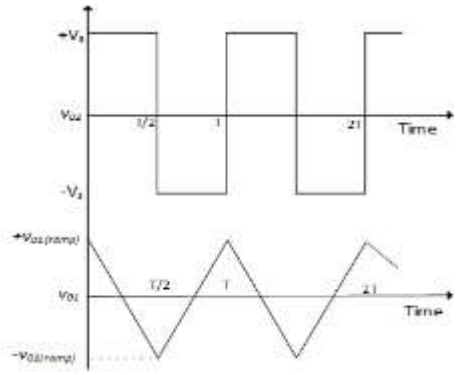

Fig. 4. Graphical representation of Square/Triangle wave of the proposed waveform generator

Consider the Fig. 1 and 2; the proposed interface circuit works as follows: CCII+ (A) is an Integrator, while CCII+ (B) is a hysteresis comparator. CCII+ (B) generates the output square wave signal v_{02} by converting the saturation current i_{z2}, into saturation voltage ($v_{02} = \pm V_s$) through resistance R_2 and R_3. A copy of the same output v_{02} is applied at the input node Y of CCII+ (A); this signal is converted in current i_{x1} through CCII+ (A), which flows through capacitor to generate the triangular waveform.

The proposed circuit generates the square/triangular waveform using two commercial second generation current conveyors AD844 and some passive components. Assuming the ideal condition of AD844AN as reported in [12] and referring to the notation of Fig. 3, one can write the network equation as

$$i_{x1} = i_{z1} \tag{3}$$

$$i_{x2} = i_{z2} \tag{4}$$

$$i_{x2} = \frac{v_{02} - v_{01}}{R_2} \tag{5}$$

The output voltage of CCII+ (B), v_{02} can be expressed as

$$v_{02} = i_{x2}.R_3 \tag{6}$$

Manipulating equation (3) to (5) we can write the voltage v_{01} as

$$v_{01} = v_{02}\left(\frac{R_3 - R_2}{R_3}\right) \tag{7}$$

v_{02} is a saturated square wave signal as shown in figure. The saturated output voltage level of CCII+ (B) is $+V_s$ for positive ramp signal and $-V_s$ for negative going ramp signal. Thus, from (7) we can obtain the peak to peak voltage of triangular wave expressed as

$$v_{01(P-P)} = 2V_s\left(\frac{R_3 - R_2}{R_3}\right) \tag{8}$$

A portion of Voltage v_{02} of CCII+ (B) is copied to high impedance node Y of CCII+ (A) which produces a current i_{x1}, expressed as

$$i_{x1} = v_{02}/R_1 \tag{9}$$

This current is then passed through the capacitor C connected at node Z, generates voltage v_{01}, expressed as

$$v_{01} = i_{z1}.X_c \tag{10}$$

The output voltage v_{01} of CCII+ (A) switches from $-v_{01(ramp)}$ to $+v_{01(ramp)}$, as the slope of v_{01} switches from negative to positive and vice versa in every half of the time period. Thus, using basic current conveyor properties and by manipulating equation (9) and (10), we can conclude the output triangular wave of CCII+ as

$$v_{01} = \frac{1}{R_1 C}\int_0^{\frac{T}{2}} v_{02}.dt = \frac{V_s}{2R_1 C}T \tag{11}$$

Finally, the expression of time period T is:

$$\mathrm{T} = 4R_1 C\frac{R_3 - R_2}{R_3} \tag{12}$$

From Equ. (12), the circuit sensitivity, for example, in capacitive sensor application, can be set by choosing suitable values of resistances R_1, R_2, and R_3. The Resistor R_1 and capacitor C can be replaced with a resistive or capacitive sensor, respectively, while other passive components allow us to set the interface sensitivity of the interface.

Considering the practical model of commercial current conveyor AD844, the parasitic components of node X, R_{XB} and R_{XA} will modify the equation (11) and (12) as

$$v_{01} = v_{02}\left[\frac{R_3 - (R_2 + R_{XB})}{R_3}\right] \tag{13}$$

$$\mathrm{T} = 4\,C(R_1 + R_{XA})\left[\frac{R_3 - (R_2 + R_{XB})}{R_3}\right] \tag{14}$$

IV. Experimental Results

To demonstrate the validity of proposed interface, experimental measurements were conducted on the fabricated prototype board using commercially available AD844 (with a DC supply of ±9V) as CCII and samples of passive components, experimental results once again confirmed theoretical expectations, showing a good linearity in wide dynamic range which covers a large number of commercial sensors (e.g. Humidity, pressure). All discrete passive components have been first measured using an LCR meter (Agilent 4294A) and found to be in the form of ±3% tolerance. A typical waveform of square/triangle wave is presented on an oscilloscope screen as shown in figure 5, obtained with R_2 = 820Ω, R_3 = 1kΩ, R_1= 100k, C= 1nF and a supply voltage of ±9 V.

In order to test the tunability of the interface circuit against the passive components R_1 and C, oscillation period was observed. Two sets of experiments have been performed for this purpose.

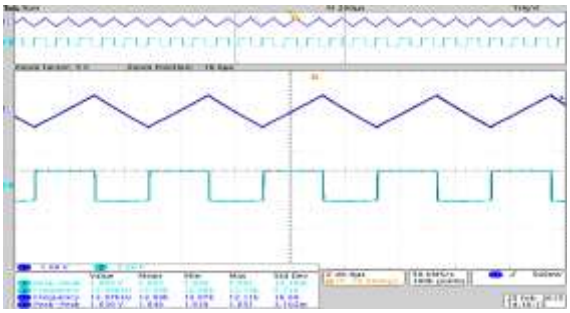

Fig. 5. Measured output at V_{01} (Triangular wave) and V_{02} (Square wave) from the built circuit

In the first experiment, the variation of oscillation period was observed against capacitance C, choosing other parameters as R_2=680Ω, R_3=1kΩ and R_1= 40kΩ. Tests conducted on the interface circuit have demonstrated that the

circuit is able to follow the capacitive variation in a wider estimation range of of about more than 2.5 decades (500pF to 200nF), maintaining a percentage relative error of lower than 8% as shown in Fig. 6.

Similarly, for Resistnace R_1, the parameters selected were R=740Ω, R_2=1kΩ and C = 100pF. Through this approach we have been able to determine about 1.5 resistive variation decades ([50kΩ to 2MΩ]) with a percentage relative error within 8% as represented in Fig. 7. Thus the prototype board demonstrated the behavior of the interface electronics circuit and display a good agreement with theoretical expectation for both capacitive and resistive sensor elements

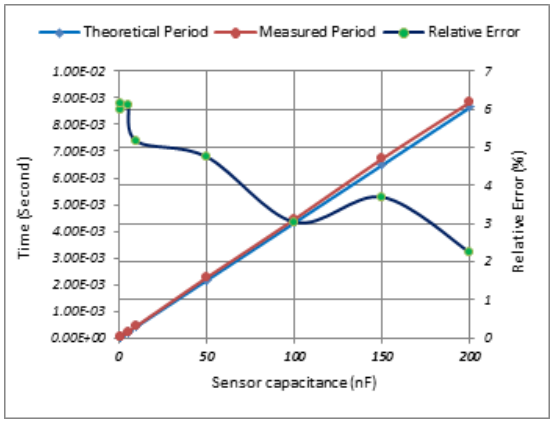

Fig. 6. Variation of time period against capacitor C

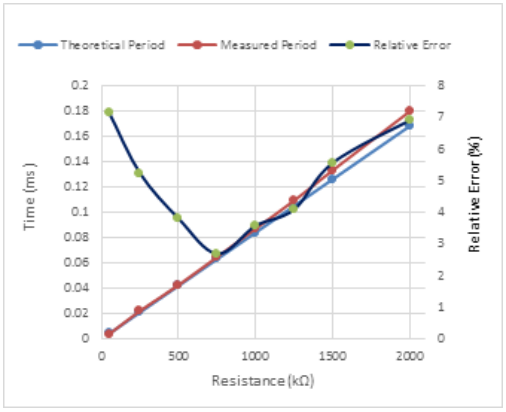

Fig. 7. Variation of time period against resistor R1

V. Experimental Results with Fabricated Capacitive Humidity Sensor

In order to test the validity of the proposed circuit in real time applications, a capacitive humidity sensor is fabricated and tested with the proposed interface circuit. The inter-digital electrode type capacitive humidity sensor fabricated on an alumina substrate [15]. A gold electrode was printed on alumina substrate using manual screen printing equipment. The substrate was then fired at 900ºC for about 1 Hours. The resultant substrate was then dipped several times in Sol-Gel solution prepared using γ–Al_2O_3 film with the help of Dip Coater [16]. Care should be taken while deciding the thickness of the film, if the thickness is larger the sensitivity of the device will be reduced and if the thickness is smaller than two electrodes may easily short.

The interface circuit was then integrated with the fabricated humidity sensor. A robust measurement setup is used to achieve a reliable and accurate response of the sensor to the different concentration of relative humidity. Capacitive sensor is placed in a circular shaped steel test chamber of 10cm height and 5cm diameter fitted in series with commercial relative humidity meter. A mixture of dry nitrogen gas and water bubbler was used to obtain the humidity content at RH level.

The Capacitive humidity sensor was simultaneously tested by interface electronic circuit and impedance analyzer at standard RH level. The output frequency of the generated square/triangular wave signal is inversely proportional to relative humidity and thus the time period is directly related to the humidity level. The output period/frequency of the proposed interface with standard humidity level is shown in Fig. 9.

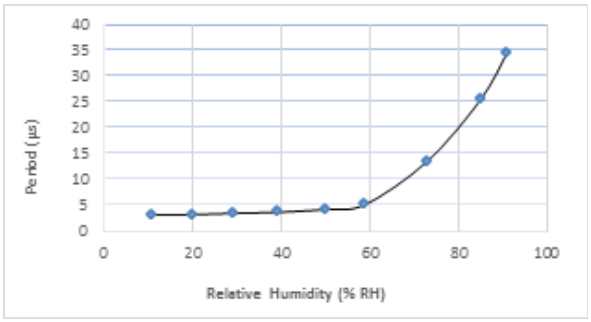

Fig. 9. Variation in period of the interface circuit with relative humidity

Finally, in order to highlight the advantages and validity of the proposed relaxation oscillator, a detailed comparison with other current mode relaxation oscillator proposed in the literature has been presented in Table 1. In particular, it is possible to highlight that the proposed oscillator provides a high oscillation frequency and wide measurement range.

VI. Conclusion

In this paper, a CCII-based square/triangle wave generator as a versatile interface for capacitive and resistive sensor has been presented and analyzed completely. It is based on current mode approach instead of classical voltage one, having a simple circuit topology implemented by only two CCIIs, so it is suitable for integration on a chip using CMOS technology with low power low voltage characteristics. Experimental measurements confirm the good linearity and wide measurement range of the interface. In order to confirm the validity of the proposed interface, a capacitive humidity sensor is fabricated and tested with the circuit. The proposed interface circuit shows good response with humidity sensor. Compared with other current feedback operational amplifier and voltage mode operational amplifier the present oscillator enjoys the following advantages; wide dynamic range, high

frequency of operation, good linearity, power consumption.

ACKNOWLEDGMENT

The authors would like to thank Prof. G. Ferri for the inspiration to work on current conveyor for sensor interfacing applications. The authors would like to thank Dr. Chandra Shekhar director CSIR-CEERI for inspiration, guidance and support.

REFERENCES

[1] A. Sedra and K. Smith, "Microelectronic Circuits," New Delhi, Oxford Univ. Press, 1998, pp. 1002-1005.

[2] A.D. Marcellis and G. Ferri, Analog circuit and system for voltage-mode and current-mode sensor interfacing application, New Delhi: Springer, 2011.

[3] R. Senani, D. Bhaskar and A. Singh, 'Current Conveyors' variant, applications and hardware implementations, New York: Springer, 2015.

[4] T. Islam, j. A. Anwar Ulla Khan and M. Z. U. Rahman, "A Digital Hygrometer for Trace Moisture Neasurement," *IEEE Trans. Instrum. Meas.,* vol. 61, pp. 5599-5605, Oct 2014.

[5] M.T. Abuelma'atti and M.A. Al-absi, "A Current conveyor-based relaxation oscillator as a versatile interface for capacitive and resistive sensors," *Int. J. Electron,* vol. 92, no. 8, pp. 473-477, 2005.

[6] P. Bruschi, N. Nizza and M. Piotto, "A Cuurent-Mode, Dual Slope, Integrated Capacitacne-to-Pulse Duration Converter," *IEEE Journal of Solid-State Circuits,* vol. 42, no. 9, pp. 1884-1891, Sept. 2007.

[7] G. D. Cataldo, G. Palumbo and S. Pennisi, "A Schmit trigger by means of a CCII+," *Int. J. Circuit Theory Appl,* vol. 23, pp. 161-165, Mar. 1995.

[8] A. D. Marcellis, C. D. Carlo, G. Ferri and V. Stornelli, "A CCII-Based wide frequency range square wave generator," *Int. Journal Circuit Theory,* pp. 1-13, March 2013.

[9] A.D. Marcellis, C.D. Carlo, G. Ferri and V. Stornelli, "A CCII-based wide frequency range square waveform generator," *Int. J. Circuit Theory Appl,* vol. 41, pp. 1-13, 2013.

[10] J. Samitier, M. Puig-Vidal, S. A. Bota, C. Rubio, S. K. Siskos and T. Laopoulos, "A Current-Mode Interface Circuit for a Poezoresistive Pressure Sensor," *IEEE Trans. Instrum. Meas.,* vol. 47, pp. 708-710, June 1998.

[11] D. Pal, A. Srinivasulu, B. B. Pal, A. Demosthenous and B. Das, "Current Conveyor-Based Square/Triangular Wave Generator With Improved Linearity," *IEEE trans. Instrum. Meas.,* vol. 58, no. 7, pp. 2174-2180, JULY 2009.

[12] Datasheet, AD844, 60 MHz, 2000 V/µs Monolithic Op Amp, Analog Devices, 2013, [online]. Available http://www.analog.com/media/en/technical-documentation/data-sheets/AD844.pdf,

[13] K. Smith and A. Sedra, "The current conveyor- A new building block," *IEEE Proc.,* vol. 56, pp. 1368-1369, May 1968.

[14] A. Sedra and K. Smith, "A second generation current conveyor and its applications," *IEEE Trans.Circuit Theory,* Vols. CT-17, pp. 132-134, Feb. 1970.

[15] T. Islam and L. Kumar and S.A. Khan, "A novel sol-gel yhin film porous alumina based capacitive sensor for measuring trace moisture in the range of 2.5 to 25 ppm," *Sens. Actuators B,* vol. 173, pp. 377-384, 2012.

[16] L. Kumar, D. Saha, S.A. Khan, K. Saha and T. Islam, "A medium range hygrometer using nano-porous thin film of Al2O3 with electronic phase detection," *IEEE Sensors Journal,* vol. 12, no. 5, pp. 1625-1632, 2012.

Table 1: - Comparison with Existing Literature

Characteristics	**This Solution**	**[11]**	**[8]**	**[5]**
Number and Kind of active components	2 CCII+	2 CCII+	2 CCII+	1 CCII+
Number and kind of passive components	4(3 Res+1Cap)	4(1 Cap +2 Res)	6 (1 Cap+5 Res)	4 (3 Res + 1 Cap)
Output Signal	Square and Triangular wave	Square and triangular wave	Square Wave	Square and triangular wave
Frequency Range	202 kHz	225kHz	737kHz (CMOS implementation)	100kHz
Relative Error	<8%	<5%	Not Mentioned	Not mentioned
Resistance variation range	50kΩ to 2MΩ	2 kΩ to 100 kΩ	20kΩ to 100kΩ	10 kΩ to 100 kΩ
Capacitance Variation range	50pF to 500nF	500pF to 10µF	1pF to 1µF	100pF to 700pF
Testing with Sensor	Yes	No	No	No